Cost Comparison of New DC Resource Connections to Railway MVDC vs. HVAC Networks

Laurent Cornaggia, Olivier Despouys, Hélène Clemot, Robin Girard, Panagiotis Andrianesis

Cost Comparison of New DC Resource Connections to Railway MVDC vs. HVAC Networks

Laurent Cornaggia
Olivier Despouys
Hélène Clemot
Research and Development
Réseau de Transport d'Électricité (RTE)
Paris, France
{first-name.last-name}@rte-france.com

Laurent Cornaggia
Robin Girard
Centre PERSEE
Mines Paris - PSL University
Paris, France
robin.girard@minesparis.psl.eu

Panagiotis Andrianesis
Department of Wind and Energy Systems
Technical University of Denmark
Kgs. Lyngby, Denmark
panosa@dtu.dk

***Abstract*—The proliferation of Direct Current (DC) resources presents significant challenges for their connection to the grid, but also opportunities for new connection options, such as Medium Voltage DC (MVDC) networks. Railway MVDC (R-MVDC) networks are among potential candidates for new DC resource connections. As such, DC resources that are geographically located near an R-MVDC network may either connect to the latter or to the closest High Voltage Alternating Current (HVAC) network. In this paper, we provide a comparison framework for both connection options based on a detailed cost analysis that considers a high fidelity model for the R-MVDC network embedding DC resources that are optimally scheduled. Our numerical illustrations considering a hybrid power plant (solar plus battery) and an R-MVDC network from the literature provide useful insights on the impact of several parameters (e.g., converter ratings and characteristics) on the comparison outcome.**

***Index Terms*—Railway MVDC networks, DC resource connection and optimization, cost-benefit analysis.**

I. Introduction

Direct Current (DC) resources are assuming a growing role in the sustainable energy transition, as they embed technologies, e.g., electrolyzers, data centers, solar power plants, which are expected to be massively deployed in the future. In addition, the progress in converter technology has increased the interest in Medium Voltage DC (MVDC) power networks [1], [2]. Existing 1.5 kV railway MVDC, hereinafter referred to as "R-MVDC" networks, could be upgraded to 9 kV [3], allowing for lower losses [4] and less substations along the train line. Such networks are natural candidates for connecting new medium-sized DC resources, which may be geographically constrained, e.g., solar power plants in land sites near the train line, data centers near optic fiber connections, electrolyzers near hydrogen consumers. Hence, the cost comparison of connecting new DC resources to either the existing High Voltage Alternating Current (HVAC) network, hereinafter referred to as "HVAC connection," or to the R-MVDC network, hereinafter referred to as "R-MVDC connection," is thus becoming more and more relevant.

There are several studies that compare point-to-point AC and DC transmission [5], [6]. In particular, [7] considered the distance beyond which the power losses of an MVDC point-to-point transmission become lower compared to an AC connection. In prior work [8], we extended [7] to account for time-varying load profiles and total costs of equipment (converters, lines) and electricity. We further provided useful insights on the connection of new DC resources to existing networks in terms of network-related costs (upgrades required or avoided, impact on network losses) and particularly the MVDC network main AC/DC converter rating. Our work [8] was motivated by an R-MVDC network and a flexible DC resource (solar plus battery), however, we neither modeled the R-MVDC network nor we detailed the impact of the new DC resource on the R-MVDC network itself.

In this paper, our focus shifts to the detailed representation of the R-MVDC and DC resource modeling and optimization. We provide a model for the R-MVDC network flows and voltages, considering train demands, and a DC resource optimization problem, which respects the R-MVDC network constraints (e.g., on voltages) and takes into consideration the impact on the R-MVDC network losses and on the equipment costs. We further detail the cost components that allow us to compare the HVAC and R-MVDC connections, and we illustrate the comparison on an R-MVDC network from the literature [3], and a DC resource (solar plus battery), accounting for the interaction of the DC resource with the train profiles and the R-MVDC network.

The main contribution of this paper is two-fold. First, we evaluate the impact of a new DC resource connection to an R-MVDC network, considering optimized DC resource schedules while taking into account R-MVDC network constraints in a high fidelity R-MVDC network model. Second, we provide a detailed cost comparison framework for evaluating new DC resource connections (R-MVDC versus HVAC).

The remainder of the paper is organized as follows. Section II details the topology for both connection options, and presents the models for the R-MVDC network and the DC resource optimization. Section III presents the methodology for the cost comparison between the different options. Section IV discusses a numerical illustration from an instance of an R-MVDC network and a hybrid power plant. Section V

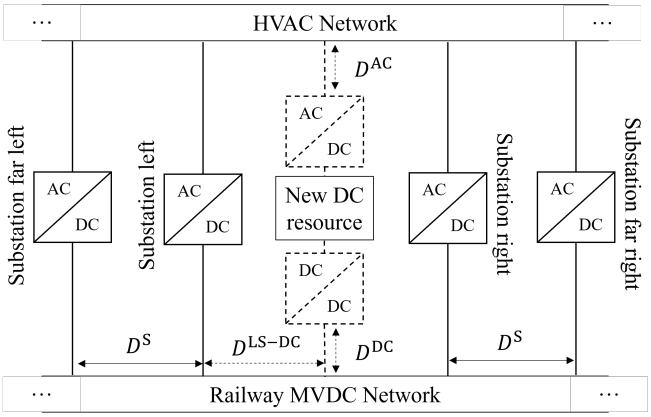

Fig. 1. Connection options for a new DC resource.

concludes and provides further research directions.

II. R-MVDC Network and DC Resource Models

In this section, we provide the topology of the networks and the new DC resource connection options (in Subsection II-A), the R-MVDC network model (in Subsection II-B), and the DC resource optimization problem (in Subsection II-C).

A. Topology and Connection Options

We consider a DC resource that is located between two substations (left and right) connecting the HVAC network and the R-MVDC network, through AC/DC converters, as shown in Fig. 1. In order to account for the trains outside the two (left and right) substations, we included in Fig. 1 the neighboring substation at each side, i.e., a far left and a far right substation. Without loss of generality, we assumed for simplicity that the distance between two neighboring substations is equal to D^{S}.

We consider the following two connection options.

1) HVAC Connection: The DC resource is connected to the HVAC network through an AC/DC converter and an HVAC line of length D^{AC}. Under such a connection, and given the sizes of the DC resources, it is reasonable to assume that the impact of this new connection on the HVAC network flows (and therefore losses) is minimal and can be neglected.

2) R-MVDC Connection: The DC resource is connected to the R-MVDC network through a DC/DC converter and an MVDC line of length D^{DC}. The distance between the connection to the R-MVDC (of the same type to the trains, i.e., between the catenary and the rail) and the left substation is denoted by $D^{\text{LS-DC}}$. Under such a connection, the sizes of the DC resources can become comparable to the loads of the trains, and hence, the impact of this new connection on the R-MVDC network flows (and losses) *cannot* be neglected.

B. R-MVDC Network Model

Let $\mathcal{N}_t = \{1, \dots, N_t\}$ denote the set of "devices," indexed by n, which are connected between the left and the right substation in Fig. 1, at time t. We use the term "devices" to refer to both trains (moving) and DC resources (static). For simplicity, we assume all devices are connected to one catenary of linear resistance R^{c}, and one rail of linear resistance R^{r}. The leakage conductance between rail and earth is neglected. Similarly to [3], [4], we represent a substation as an ideal voltage generator V^{S} plus an equivalent internal resistance R^{eq}. For the purposes of our analysis, we consider a time granularity, t, of 1 minute, and we denote the position of each device n at time t, by $x_{n,t}$. Since the trains are moving, the ordering of the devices may change every minute. We therefore introduced an ordered set of devices, and substations, (henceforth referred to as elements) starting from the left substation, indexed by 0, and ending at the right substation, indexed by $N_t + 1$, for which we use the set $\mathcal{K}_t = \{0, \dots, k-1, k, \dots N_t + 1\}$, indexed by k. With some abuse of notation, we denote by $x_{k,t}$ the position of the k-th element that one meets when starting from the left substation ($k = 0$) and moving towards the right substation ($k = N_t+1$). For the sake of a uniform notation, we keep the time index even when referring to the two (left and right) substations, i.e., $x_{0,t}$ and $x_{N_t+1,t}$, or to static devices. Evidently, the distance between the two substations is given by $x_{N_t+1,t} - x_{0,t} = D^{\mathrm{S}}$, $\forall t$, whereas for a static DC resource, say n^{DC}, the distance from the left substation is given by $x_{n^{\mathrm{DC}},t} - x_{0,t} = D^{\text{LS-DC}}$, $\forall t$ (see Fig. 1).

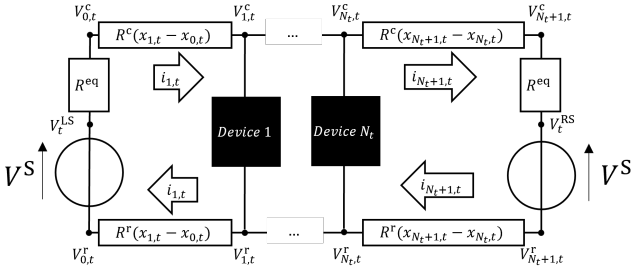

Fig. 2. Power model for the R-MVDC.

Let $V^{\mathrm{c}}_{k,t}$ and $V^{\mathrm{r}}_{k,t}$ denote the voltages of the catenary and the rail, respectively, at the k-th position (i.e., the position of the k-th ordered element), at time t. Let V^{LS}_t and V^{RS}_t denote the voltages inside the left and right substations, respectively, before the internal resistance. Let $i_{k,t}$ denote the symmetric intensity (the symmetry can be assessed via a recurrence demonstration) circulating in the rail and the catenary from left to right (with k indicating the point towards which the intensity is directed). We can then represent the model of the R-MVDC network as pictured in Fig. 2, which is described by the following equations, $\forall t$.

$$i_{k,t} R^{\mathrm{c}}(x_{k,t} - x_{k-1,t}) = V^{\mathrm{c}}_{k,t} - V^{\mathrm{c}}_{k-1,t}, \quad \forall k \in \mathcal{K}_t \setminus \{0\}, \tag{1}$$

$$i_{k,t} R^{\mathrm{r}}(x_{k,t} - x_{k-1,t}) = V^{\mathrm{r}}_{k-1,t} - V^{\mathrm{r}}_{k,t}, \quad \forall k \in \mathcal{K}_t \setminus \{0\}, \tag{2}$$

$$V^{\mathrm{LS}}_t - V^{\mathrm{c}}_{0,t} = R^{\mathrm{eq}}\, i_{1,t}, \tag{3}$$

$$V^{\mathrm{c}}_{N_t+1,t} - V^{\mathrm{RS}}_t = R^{\mathrm{eq}}\, i_{N_t+1,t}, \tag{4}$$

$$V^{\mathrm{LS}}_t - V^{\mathrm{r}}_{0,t} = V^{\mathrm{S}}, \tag{5}$$

$$V^{\mathrm{RS}}_t - V^{\mathrm{r}}_{N_t+1,t} = V^{\mathrm{S}}, \tag{6}$$

$$V^{\mathrm{r}}_{0,t} = 0. \tag{7}$$

Eqs. (1) and (2) describe the voltage drop between two adja-

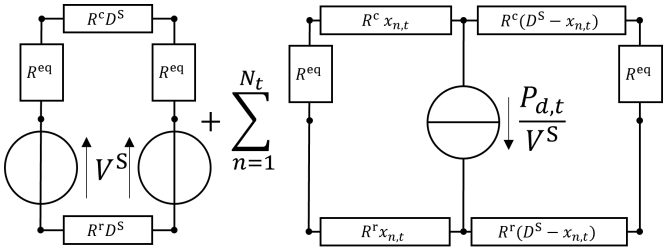

Fig. 3. Superposition principle using the ideal current source approximation.

cent positions of the catenary and rail, respectively. Eqs. (3) and (4) describe the voltage drop at the substation terminals, whereas (5) and (6) describe the ideal voltage source, at the left and the right substation, respectively, Eq. (7) sets a convention to have a zero voltage at the rail just before the connection to the left substation converter.

The power consumed by the k-th element (device), denoted by $P_{k,t}$ (positive for consumption, negative for production) is given by:

$$P_{k,t} = (V^{\mathrm{c}}_{k,t} - V^{\mathrm{r}}_{k,t})(i_{k,t} - i_{k+1,t}),\ \forall k \in \mathcal{K}_t \setminus \{0, N_t+1\}. \tag{8}$$

However, assuming that the voltage difference between the rail and the catenary is close to V^{S}, we can use a linear approximation of the quadratic equation (8) given by:

$$P_{k,t} = V^{\mathrm{S}}(i_{k,t} - i_{k+1,t}),\ \forall k \in \mathcal{K}_t \setminus \{0, N_t+1\}, \tag{9}$$

which corresponds to an ideal current source representation of the devices, of intensity $\frac{P_{k,t}}{V^{\mathrm{S}}}$.

We analytically solve the system of linear equations (1)–(7), and (9), using the superposition principle by decomposing the solution into the solution with only the ideal voltage sources (where there is no intensity, the voltage at the catenary is V^{S} and the voltage at rail is 0) and the solutions considering only one device at a time (where the intensities and voltage drop along the catenary and the rails can be determined with the relative ratios of the resistances) as shown in Fig. 3.

Setting $x_{0,t} = 0$, thus $x_{N_t+1,t} = D^{\mathrm{S}}$, the intensities $i_{k,t}$ can be written as the sum of intensities found only with one current source $i^{\mathrm{only}}_{n,t}(x)$ at the position $x = x_{k,t}$, as follows:

$$i_{k,t} = \sum_{n=1}^{N_t} i^{\mathrm{only}}_{n,t}(x_{k,t}), \tag{10}$$

where the intensity caused by device n, only, generating current $\frac{P_{n,t}}{V^{\mathrm{S}}}$ at a position $x_{n,t}$ of the circuit, $i^{\mathrm{only}}_{n,t}(x)$, can be analytically computed using the current division, as follows:

$$i^{\mathrm{only}}_{n,t}(x \le x_{n,t}) = \left(\frac{P_{n,t}}{V^{\mathrm{S}}}\right) \frac{R^{\mathrm{eq}} + (R^{\mathrm{r}} + R^{\mathrm{c}})(D^{\mathrm{S}} - x_{n,t})}{2R^{\mathrm{eq}} + D^{\mathrm{S}}(R^{\mathrm{r}} + R^{\mathrm{c}})}, \tag{11}$$

$$i^{\mathrm{only}}_{n,t}(x > x_{n,t}) = -\left(\frac{P_{n,t}}{V^{\mathrm{S}}}\right) \frac{R^{\mathrm{eq}} + (R^{\mathrm{r}} + R^{\mathrm{c}})x_{n,t}}{2R^{\mathrm{eq}} + D^{\mathrm{S}}(R^{\mathrm{r}} + R^{\mathrm{c}})}. \tag{12}$$

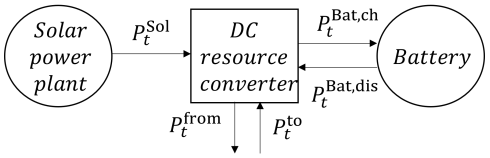

Fig. 4. DC resource representation.

Using (10), the catenary and rail voltages can be computed by recursively applying (1) and (2), respectively. Applying also (3), (5), and (7), we obtain:

$$V^{\mathrm{c}}_{k,t} = V^{\mathrm{S}} - R^{\mathrm{eq}} i_{1,t} - \sum_{j=1}^{k} R^{\mathrm{c}}(x_{j,t} - x_{j-1,t}) i_{j,t}, \tag{13}$$

$$V^{\mathrm{r}}_{k,t} = \sum_{j=1}^{k} R^{\mathrm{r}}(x_{j,t} - x_{j-1,t}) i_{j,t}. \tag{14}$$

C. DC Resource Optimization Model

The DC resource may be a non-flexible load or generation such as a data center or a solar power plant, or it can embed some flexibility (e.g. load shifting, load shedding, storage capacity), with or without a power consumption or production.

In this work, we consider the combination of a solar power plant and a storage facility, but our analysis remains still relevant for other types of DC resources. Let P^{Sol}_t denote the solar power plant generation at time t, with $\bar{P}^{\mathrm{Sol}}_t$ denoting the available production at time t. The battery parameters are denoted by $P^{\mathrm{Bat,ch}}_t$ and $P^{\mathrm{Bat,dis}}_t$ for the charging and discharging power, respectively, at time t, $\bar{P}^{\mathrm{Bat}}$ for the battery power limit, $\eta^{\mathrm{Bat,ch}}$ and $\eta^{\mathrm{Bat,dis}}$ for the charging and discharging efficiencies, respectively, e^{Bat}_t for the battery state of energy at time t, and $E^{\mathrm{Bat}}_{\min}$ and $E^{\mathrm{Bat}}_{\max}$ for the minimum and maximum energy limits, respectively. Let P^{from}_t denote the power flowing from the DC resource to the network after its converter, and P^{to}_t denote the power flowing to the DC resource from the network before its converter. The DC resource converter has a constant efficiency, η^{DCR}, and maximum power $\bar{P}^{\mathrm{DCR}}$. The battery and the solar panel converters are not modelled since they are already taken into account through the efficiency of the battery and the expected production of the solar power plant.

The DC resource representation is illustrated in Fig. 4, and is modeled as follows, $\forall t$:

$$\frac{1}{\eta^{\mathrm{DCR}}} P^{\mathrm{from}}_t - \eta^{\mathrm{DCR}} P^{\mathrm{to}}_t = P^{\mathrm{Sol}}_t - P^{\mathrm{Bat,ch}}_t + P^{\mathrm{Bat,dis}}_t, \tag{15}$$

$$0 \le P^{\mathrm{Sol}}_t \le \bar{P}^{\mathrm{Sol}}_t, \tag{16}$$

$$e^{\mathrm{Bat}}_t = e^{\mathrm{Bat}}_{t-1} + \eta^{\mathrm{Bat,ch}} p^{\mathrm{ch}}_t - \frac{1}{\eta^{\mathrm{Bat,dis}}} p^{\mathrm{Bat,dis}}_t, \tag{17}$$

$$E^{\mathrm{Bat}}_{\min} \le e^{\mathrm{Bat}}_t \le E^{\mathrm{Bat}}_{\max}. \tag{18}$$

$$0 \le p^{\mathrm{Bat,ch}}_t \le b^{\mathrm{Bat}}_t \bar{P}^{\mathrm{Bat}}, \tag{19}$$

$$0 \le p^{\mathrm{Bat,dis}}_t \le (1 - b^{\mathrm{Bat}}_t) \bar{P}^{\mathrm{Bat}}, \tag{20}$$

$$0 \le P^{\mathrm{to}}_t \le b^{\mathrm{DCR}}_t \bar{P}^{\mathrm{DCR}}, \tag{21}$$

$$0 \le P^{\mathrm{from}}_t \le (1 - b^{\mathrm{DCR}}_t) \bar{P}^{\mathrm{DCR}}. \tag{22}$$

Eq. (15) represents the power balance at the converter. Constraint (16) enforces the limits of the solar production (allowing for potential curtailment). Eq. (17) defines the battery state of charge, whereas (18) enforces the battery state of charge limits. Constraints (19)–(20) and (21)–(22) enforce power limits on the power of the battery and the DC resource, respectively. Binary variables b_t^{Bat} (1: charging; 0: discharging), and b_t^{DCR} (1: $P_t^{\text{from}} = 0$, 0: $P_t^{\text{to}} = 0$) ensure that the battery is not charging and discharging simultaneously, and similarly, the power is not flowing from and to the DC resource simultaneously. To ensure consistency in a daily simulation, we assume the battery initial state of charge is $e_0^{\text{Bat}} = E_{\min}^{\text{Bat}}$.

Let c_t^E denote the cost of electricity for time t. The DC resource optimization problem depending on chosen connection option is provided below.

The cost of the DC resource is given by:

$$C^{\text{DCR}} = \sum_t c_t^E (P_t^{\text{to}} - P_t^{\text{from}}) \tag{23}$$

For the HVAC connection, the optimal DC resource schedule is given by the following Mixed Integer Linear Programming (MILP) problem:

$$\textbf{DCR}^{\text{HVAC}}: \ \min \ (23) \text{ s.t. } (15)-(22). \tag{24}$$

For the R-MVDC connection, we require additional constraints. Let k_t^{DCR} denote the position of DC resource at time t. Using (10), we can express $i_{k,t}$ as the sum of the intensity due to the DC resource, $i^{\text{only}}_{k_t^{\text{DCR}},t}(x_{k,t})$ (variable), written as $i^{\text{DCR-only}}_{k,t}$ for short, and all other intensities due to other devices (trains) connected to the R-MVDC (parameters), as follows:

$$i_{k,t} = i_{k,t}^{\text{DCR-only}} + \sum_{k' \in \mathcal{K}_t \setminus \{k_t^{\text{DCR}}\}} i^{\text{only}}_{k',t}(x_{k,t}), \tag{25}$$

Using (11) and (12), and replacing $P_{n,t}$ by P_t^{from} and P_t^{to}, we can define $i_{k,t}^{\text{DCR-only}}$ as follows:

$$i_{k,t}^{\text{DCR-only}} = \frac{P_t^{\text{to}} - P_t^{\text{from}}}{V^{\text{S}}} \delta_{k,t}, \tag{26}$$

where $\delta_{k,t}$ is a parameter that is given by:

$$\delta_{k,t} = \frac{R^{\text{eq}} + (R^{\text{r}} + R^{\text{c}})(D^{\text{S}} - D^{\text{LS-DC}})}{2R^{\text{eq}} + (R^{\text{r}} + R^{\text{c}})D^{\text{S}}}, \quad k \le k_t^{\text{DCR}}, \tag{27a}$$

$$\delta_{k,t} = -\frac{R^{\text{eq}} + (R^{\text{r}} + R^{\text{c}})D^{\text{LS-DC}}}{2R^{\text{eq}} + (R^{\text{r}} + R^{\text{c}})D^{\text{S}}}, \quad k > k_t^{\text{DCR}}. \tag{27b}$$

Other device (train) intensities are also calculated using (11), (12), since their power $P_{n,t}$ is known.

Let $V_{\min}^{\text{c}}$ and $V_{\max}^{\text{c}}$ ($V_{\min}^{\text{r}}$ and $V_{\max}^{\text{r}}$) be the catenary (rail) minimum and maximum voltage limits, respectively. Each element k should respect these limits, i.e., $\forall t$:

$$V_{\min}^{\text{c}} \le V_{k,t}^{\text{c}} \le V_{\max}^{\text{c}}, \quad \forall k \in \mathcal{K}_t \tag{28}$$

$$V_{\min}^{\text{r}} \le V_{k,t}^{\text{r}} \le V_{\max}^{\text{r}}, \quad \forall k \in \mathcal{K}_t. \tag{29}$$

In Fig. 5, we present two nodes (black boxes) at the R-MVDC network, where we consider the power balance. Let $P_t^{\text{LS,from}}$ ($P_t^{\text{RS,from}}$) denote the power flowing *from* the LS (RS) substation converter to the R-MVDC left (right) node. Similarly, let $P_t^{\text{LS,to}}$ ($P_t^{\text{RS,to}}$) denote the power flowing *to* the LS (RS) substation converter from the R-MVDC left (right) node. Let P_t^{FLS} (P_t^{FRS}) denote the power flowing from the left (right) R-MVDC node to the far left (far right) substation. Using the intensities at the two nodes, $i_{1,t}$ (left substation) and $i_{N_t+1,t}$ (right substation), the power balance at the two nodes is described as follows:

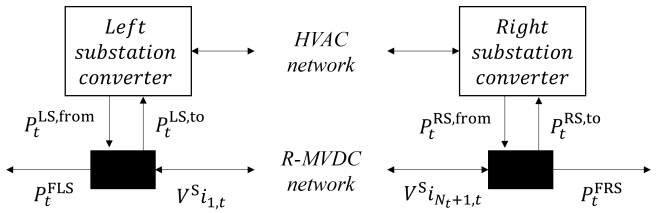

Fig. 5. Substation converters equilibrium representation.

$$P_t^{\text{LS,from}} - P_t^{\text{LS,to}} = P_t^{\text{FLS}} + V^{\text{S}} i_{1,t}, \tag{30}$$

$$P_t^{\text{RS,from}} - P_t^{\text{RS,to}} = P_t^{\text{FRS}} - V^{\text{S}} i_{N_t+1,t}. \tag{31}$$

Considering also the substation converter rating, $\bar{P}^{\text{s}}$, we require that, $\forall t$:

$$0 \le P_t^{\text{LS,to}} \le \alpha b_t^{\text{LS}} \bar{P}^{\text{S}}, \tag{32}$$

$$0 \le P_t^{\text{LS,from}} \le (1 - b_t^{\text{LS}}) \bar{P}^{\text{S}}, \tag{33}$$

$$0 \le P_t^{\text{RS,to}} \le \alpha b_t^{\text{RS}} \bar{P}^{\text{S}}, \tag{34}$$

$$0 \le P_t^{\text{RS,from}} \le (1 - b_t^{\text{RS}}) \bar{P}^{\text{S}}, \tag{35}$$

where binary variables b_t^{LS} and b_t^{RS} prevent the simultaneous from/to flows, whereas α is an indicator that describes bidirectionality, i.e., (1: bidirectional, 0: monodirectional).

Taking into account the substation converter efficiency, η^{S}, the cost for supplying both the DC resource and the trains is given by:

$$C_{\text{R-MVDC}}^{\text{DCR-T}} = \sum_t c_t^E \Big(\frac{P_t^{\text{LS,from}} + P_t^{\text{RS,from}}}{\eta^{\text{S}}} - \eta^{\text{S}} \big(P_t^{\text{LS,to}} + P_t^{\text{RS,to}} \big) \Big), \tag{36}$$

Hence, summarizing for the R-MVDC connection, the optimal DC resource schedule is given by the following MILP problem:

$$\textbf{DCR}^{\text{R-MVDC}}: \ \min \ (36) \text{ s.t. } (10)-(22), (25)-(35). \tag{37}$$

III. Cost Comparison of Connection Options

In this section, we present the methodology used to compute the costs of each connection option and detail the cost components used in the comparison.

We first use the DC resource optimization model described in Subsection II-C, to obtain optimal schedules for a certain number of representative days, to account for the yearly variability in the DC resource load/generation and the electricity prices.

We then consider the costs related to the two connection options. These include the following components:

- The cost of R-MVDC Joule losses, denoted by C^{J} (in EUR/year).
- The cost of the DC resource (which embeds the losses of the DC resource converter), denoted by C^{DCR} (in EUR/year).
- The cost of supplying the train demand (which embeds the losses of the substation converters), denoted by C^{T} (in EUR/year).
- The cost of converter CAPEX and fixed OPEX, denoted by C^{C} (in EUR/year).
- The cost of the DC resource line Joule losses, denoted by c^{DCR} (in EUR/km/year).
- The cost of DC resource line CAPEX and fixed OPEX, denoted by c^{L} (in EUR/km/year).

The total costs, $\mathrm{TC}(D)$, are given by:

$$\mathrm{TC}(D) = \overbrace{C^{\mathrm{J}} + C^{\mathrm{DCR}} + C^{\mathrm{T}} + C^{\mathrm{C}}}^{C^{\mathrm{Total}}} + \overbrace{(c^{\mathrm{DCR}} + c^{\mathrm{L}})}^{c^{\mathrm{Total}}} D, \quad (38)$$

where $D = D^{\mathrm{AC}}$ for the HVAC connection and $D = D^{\mathrm{DC}}$ for the R-MVDC connection. We can then define the R-MVDC cost break-even distance $\mathrm{CBED}^{\text{R-MVDC}}$, as the distance D^{DC} at which the total costs are equal for both options, i.e., $\mathrm{TC}_{\mathrm{HVAC}}(D^{\mathrm{AC}}) = \mathrm{TC}_{\text{R-MVDC}}(D^{\mathrm{DC}} = \mathrm{CBED}^{\text{R-MVDC}})$, as follows:

$$\mathrm{CBED}^{\text{R-MVDC}} = \frac{C^{\mathrm{Total}}_{\mathrm{HVAC}} - C^{\mathrm{Total}}_{\text{R-MVDC}}}{c^{\mathrm{Total}}_{\text{R-MVDC}}} + \frac{c^{\mathrm{Total}}_{\mathrm{HVAC}}}{c^{\mathrm{Total}}_{\text{R-MVDC}}} D^{\mathrm{AC}}. \quad (39)$$

Next, we describe the calculation of each component.

1) Cost of R-MVDC Joule Losses: We compute the exact cost of Joule losses in the R-MVDC network, using the linear approximation of Eq. (9) as an initial guess to find the solutions of the quadratic system of Eq. (1)–(8), and then use:

$$C^{\mathrm{J}} = \sum_t \sum_{k=1}^{N_t+1} c^E_t (R^{\mathrm{c}} + R^{\mathrm{r}})(x_{k,t} - x_{k-1,t}) i^2_{k,t} \quad (40)$$

Note that the equivalent internal resistance of the substation converters is not taken into account in (40), as the losses of the these converters are taken into account in the cost of supply of the trains C^{T}.

2) Cost of DC Resource: It is given by (23) for both options. If negative, it represents a benefit.

3) Cost of Supplying the Train Demand: For the HVAC connection, it can be computed by the trains demand, accounting the substation converter efficiency as follows:

$$C^{\mathrm{T}}_{\mathrm{HVAC}} = \frac{1}{\eta^{\mathrm{S}}} \sum_t c^E_t \big(P^{\mathrm{FLS}}_t + P^{\mathrm{FRS}}_t + \sum_{k' \in \mathcal{K}_t \setminus \{k^{\mathrm{DCR}}_t\}} P_{k',t}\big). \quad (41)$$

For the R-MVDC connection, it is obtained by the total cost in (36) minus the cost of DC Resource C^{DCR} in (23), i.e.,

$$C^{\mathrm{T}}_{\text{R-MVDC}} = C^{\text{DCR-T}}_{\text{R-MVDC}} - C^{\mathrm{DCR}} \quad (42)$$

4) Cost of Converter CAPEX and Fixed OPEX: There are three converters that are impacted by the connection option: the AC/DC (DC/DC) hybrid converter for the HVAC (R-MVDC) connection and the two AC/DC left and right substation converters. For each converter, the cost is annualised through the formula :

$$C^{\mathrm{C}} = \sum_{i=1}^{3} \bar{P}_i \mathrm{CAPEX}^{\mathrm{C}}_i \Big(\frac{\tau^{\mathrm{C}}_i / (1+\tau^{\mathrm{C}}_i)}{1 - (1+\tau^{\mathrm{C}}_i)^{-L^{\mathrm{C}}_i}} + \mathrm{OPEX}^{\mathrm{C}}_i \Big), \quad (43)$$

where i represents the three converters, $\bar{P}_i$ the rating in MW, $\mathrm{CAPEX}^{\mathrm{C}}_i$ the investment CAPEX in EUR/MW, $\mathrm{OPEX}^{\mathrm{C}}_i$ the relative fixed OPEX in %CAPEX/year, L^{C}_i the lifetime in years, and τ^{C}_i the discount factor.

5) Cost of the DC Resource Line Joule Losses: They are computed as follows:

$$c^{\mathrm{DCR}}_{\mathrm{HVAC}} = \sum_t c^E_t R^{\mathrm{AC}} \Big(\frac{P^{\mathrm{from}}_t - P^{\mathrm{to}}_t}{U^{\mathrm{AC}} \cos\phi} \Big)^2, \quad (44)$$

$$c^{\mathrm{DCR}}_{\text{R-MVDC}} = \sum_t c^E_t 2R^{\mathrm{DC}} \Big(\frac{P^{\mathrm{from}}_t - P^{\mathrm{to}}_t}{V^c_{k^{\mathrm{DCR}}_t} - V^r_{k^{\mathrm{DCR}}_t}} \Big)^2, \quad (45)$$

where U^{AC} is the tension phase-to-phase RMS of the HVAC network, $\cos\phi$ its power factor, R^{AC} the linear resistance of the HVAC line, and R^{DC} the linear resistance of the DC line (doubled to account for the two poles of the DC line).

6) Cost of DC Resource Line CAPEX and Fixed OPEX: It is given by:

$$c^{\mathrm{L}} = \mathrm{CAPEX}^{\mathrm{L}} \Big(\frac{\tau^{\mathrm{L}} / (1+\tau^{\mathrm{L}})}{1 - (1+\tau^{\mathrm{L}})^{-L^{\mathrm{L}}}} + \mathrm{OPEX}^{\mathrm{L}} \Big), \quad (46)$$

where $\mathrm{CAPEX}^{\mathrm{L}}$ is the investment CAPEX of the line in EUR/km, $\mathrm{OPEX}^{\mathrm{L}}$ the relative fixed OPEX in %CAPEX/year, L^{L} the lifetime in years, and τ^{L} the discount factor.

IV. Numerical Illustration

In this section, we describe the test cases used for the numerical illustration (in Subsection IV-A), and we present daily and yearly results (in Subsections IV-B and IV-C, respectively).

A. Test Cases

In our numerical experiments, we use the R-MVDC network from [3], with $V^{\mathrm{S}} = 9$ kV DC and $D^{\mathrm{S}} = 100$ km. We consider both 50 passenger and 25 freight trains per day (without regenerative braking) with speeds of 160 and 120 km per hour, respectively. All trains have minimum, mean and maximum powers of 0.3, 1 and 3 MW with first and last departures at 6am and 10pm, respectively. We model train power consumption, by setting the power for each minute to either the minimum or the maximum value, ensuring that the average power aligns with the mean power to calibrate with available data on train power profiles. Catenary and rail voltages limits are $V^{\mathrm{c}}_{min} = 6$, $V^{\mathrm{c}}_{max} = 10.8$, $V^{\mathrm{r}}_{min} = -0.9$ and $V^{\mathrm{r}}_{max} = 0.9$ kV DC. The AC/DC substation converters rating is $\bar{P}^{\mathrm{S}} = 15$ MW, they are bidirectional ($\alpha = 1$), and their efficiency is $\eta^{\mathrm{S}} = 99\%$. The HVAC network voltage is

$U^{\text{AC}} = 63$ kV AC phase-to-phase RMS, with $\cos\phi = 0.95$. Linear resistances (in mΩ/km) are $R^{\text{c}} = 24$ for the catenary, $R^{\text{r}} = 17$ for the rail, $R^{\text{AC}} = 27.3$ for the HVAC line, and $R^{\text{DC}} = 21.1$ for the MVDC line. The equivalent resistance of the substation converters is $R^{\text{eq}} = 30$ mΩ.

The DC resource is located at the middle of both substations, i.e., $D^{\text{LS-DC}} = 50$ km. The rating of the bidirectional DC resource converter is $\bar{P}^{\text{DCR}} = 15$ MW and its efficiency is $\eta^{\text{DCR}} = 99\%$. The DC resource is a hybrid power plant that includes a solar plant of installed capacity 20 MWc, and a battery with maximal power $\bar{P}^{\text{Bat}} = 10$ MW, energy (capacity) limits $E^{\text{Bat}}_{\text{min}} = 0$ and $E^{\text{Bat}}_{\text{max}} = 20$ MWh, and efficiency $\eta^{\text{Bat,ch}} = \eta^{\text{Bat,dis}} = 92\%$. We obtain the solar production time series from the PECD database [9] (France 2019) and the electricity price from the ENTSO-E database (France 2019 day-ahead prices, post processed to set the minimum price at 0.1 EUR/MWh, in order to avoid using the battery as a pure resistance in case of a negative price).

The monodirectional converter CAPEX is 112.5 kEUR/MW for the AC/DC and 200 kEUR/MW for DC/DC. The bidirectional converter CAPEX are assumed to be twice their monodirectional counterpart, The lifetime of all converters is 25 years, with a fixed OPEX cost 0.5% of CAPEX/year. The CAPEX of the line to connect the DC resource is 200 kEUR/km, its lifetime is 45 years and its fixed OPEX cost is 1.5% of CAPEX/year. Discount factors are 3%.

In our numerical experiments, we consider a Base Case and 5 variants:

- **Base Case**: It uses the aforementioned values.
- **Variant 1 (2)**: It considers smaller (larger) converter ratings with $\bar{P}^{\text{S}} = \bar{P}^{\text{DCR}} = 10\,(20)$ MW.
- **Variant 3**: It considers a higher electricity price (double).
- **Variant 4**: It considers monodirectional substation converters (hence forbidding the injection of the DC resource production to the HVAC network), i.e., $\alpha = 0$.
- **Variant 5**: It considers stricter limits for the catenary voltages with $V^{\text{c}}_{\text{max}} = 9.5$ and $V^{\text{c}}_{\text{min}} = 8$ kV DC.

B. Daily Results

We indicatively represent the June 18th daily results (one-minute resolution) for the Base Case in Figs. 6–8.

In Fig. 6, we show the solar production and battery charging/discharging profile, i.e., the DC resource schedule, and the train schedule (demand). Unsurprisingly, the battery usually charges (discharges) when the electricity price is low (high).

In Fig. 7, we illustrate the minimum and maximum catenary voltage, as well as the catenary voltage at the location of the DC resource. Comparing with Fig. 6, we observe the impact of the DC resource schedule on the catenary voltages. DC resource consumption (battery charging) is associated with lower minimum catenary voltages, whereas production (solar plus battery discharging) with higher maximum catenary voltages. The catenary voltage at the location of the DC resource is in most cases close to one of one extremum of the catenary voltages (the most distant from the nominal value).

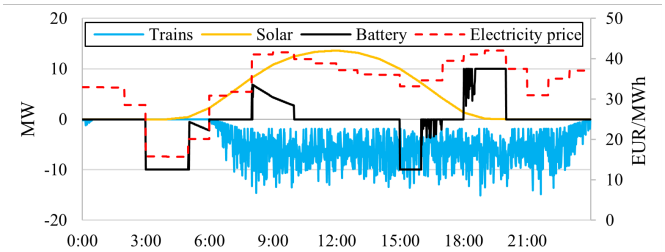

Fig. 6. DC resource and trains schedule (left axis) and electricity price (right axis).

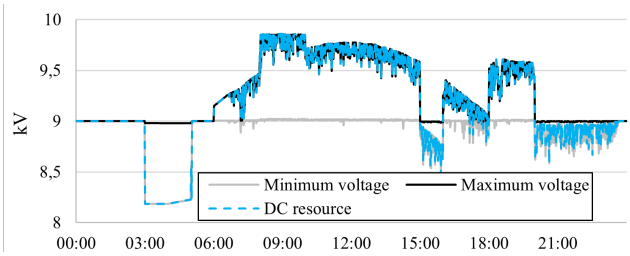

Fig. 7. Catenary voltages: minimum, maximum, DC resource location.

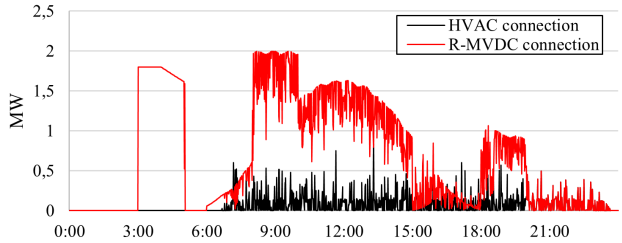

Fig. 8. R-MVDC network Joule losses for both connection options.

In Fig. 8, we illustrate the R-MVDC network Joule losses for both connections options. Evidently, the losses for the HVAC connection are due to the train profiles, whereas the (significantly higher) losses for the R-MVDC connection are due to the DC resource schedule (which adds to the train profile) — compare with Fig. 6.

C. Yearly Results

In Tables I and II, we present yearly fixed and linear costs for both connection options, for the Base Case and Variants (V.1 to V.5). Total costs (both fixed C^{Tot}, and linear c^{Tot}) are higher for the R-MVDC connection compared to the HVAC option, mainly because of the higher Joule losses, C^{J}, c^{DCR}, and converter costs, C^{C}. The cost of the DC resource C^{DCR} is higher (i.e., lower benefit) in Variant 4 (5), where the monodirectional converter (stricter voltage limits) affects the DC resource schedule.

In Fig. 9, we present the cost break-even distance (CBED), $\text{CBED}^{\text{R-MVDC}}$, i.e., the distance of the DC resource from the R-MVDC network at which the total costs are equal for both options, — see (39), versus different distances of the DC resource from the HVAC network (D^{AC}), for the Base Case and its variants. Comparing the Variants to the Base Case in Fig. 9, we can make the following remarks.

TABLE I
FIXED COSTS [KEUR/YEAR]

	Base	V. 1	V. 2	V. 3	V. 4	V. 5
C^{J}_{HVAC}	27	27	27	53	27	27
$C^{J}_{R\text{-}MVDC}$	169	141	173	339	54	124
C^{DCR}_{HVAC}	-1204	-1172	-1205	-2407	-1204	-1204
$C^{DCR}_{R\text{-}MVDC}$	-1204	-1172	-1205	-2407	-882	-1150
C^{T}_{HVAC}	1674	1674	1674	3348	1674	1674
$C^{T}_{R\text{-}MVDC}$	1673	1671	1673	3346	1665	1670
C^{C}_{HVAC}	615	410	820	615	410	615
$C^{C}_{R\text{-}MVDC}$	775	516	1033	775	570	775
C^{Total}_{HVAC}	**1112**	**938**	**1315**	**1609**	**907**	**1112**
$C^{Total}_{R\text{-}MVDC}$	**1414**	**1157**	**1674**	**2053**	**1406**	**1419**

TABLE II
LINEAR COSTS [KEUR/KM/YEAR]

	Base	V. 1	V. 2	V. 3	V. 4	V. 5
c^{L}_{HVAC}	10,9	10,9	10,9	10,9	10,9	10,9
$c^{L}_{R\text{-}MVDC}$	10,9	10,9	10,9	10,9	10,9	10,9
c^{DCR}_{HVAC}	0,1	0,1	0,1	0,3	0,1	0,1
$c^{DCR}_{R\text{-}MVDC}$	7,9	6,8	8,1	15,9	3,1	6,2
c^{Total}_{HVAC}	**11,1**	**11,0**	**11,1**	**11,2**	**11,1**	**11,1**
$c^{Total}_{R\text{-}MVDC}$	**18,9**	**17,7**	**19,0**	**26,8**	**14,0**	**17,1**

First, Variants 1 and 2 indicate that smaller converter ratings increase the CBED, i.e., increase the distance at which the R-MVDC connection is preferred, mainly due to the lower converter costs (benefiting more the R-MVDC connection). Second, Variant 3 indicates that increased electricity prices decrease the CBED, mainly due to the increased cost of Joule losses, which is higher in the R-MVDC connection. Third, Variant 4 indicates that installing monodirectional substation converters decreases the CBED, because the savings from the converter costs in Table I (HVAC: 615 - 410 = 205 vs R-MVDC = 775 - 570 = 205) do not compensate for the loss in the DC resource benefit (HVAC: 1204 - 1204 = 0 vs R-MVDC: 1204 - 882 = 322). We also observe that as the distance of the DC resource from the HVAC network (D^{AC}) increases, the CBED difference from the Base Case is reduced. The reason is that the linear costs due to Joule effects in the DCR line in the R-MVDC option are decreased (7.9 - 3.1 = 4.8). Fourth, Variant 5 shows a similar CBED for low distances of (D^{AC}), and slightly increases for higher distances, thus providing the impression that restricting catenary voltage limits might make the R-MVDC connection more favorable. Taking a closer look at Tables I and II, we observe that the total fixed costs are almost equal with the Base Case (Variant 5 has lower Joule losses but also lower DC resource benefits), but the total linear costs are lower than the Base Case (Variant 5 has lower linear DC resource line Joule losses costs). This is a result from the fact that the R-MVDC Joule losses are not embedded in the DC resource optimization problem but are calculated given the DC resource schedules (with the difference in the linear costs affecting more the higher distances — see (39)).

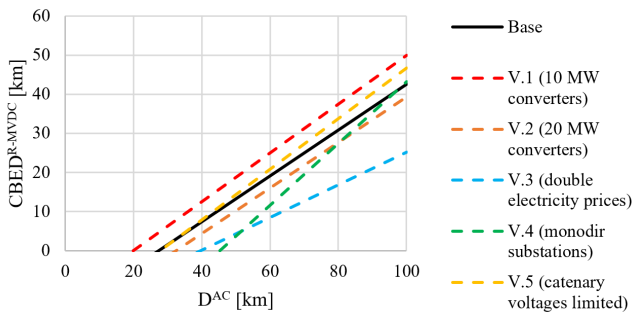

Fig. 9. R-MVDC cost break-even distance.

V. CONCLUSIONS AND FURTHER RESEARCH

In this work, we presented a framework for the cost comparison of new DC resource connections to an HVAC or an R-MVDC network. We computed the optimal schedule of a DC resource connected to a R-MVDC network, which we used to compute the various cost components for both connection options. Our numerical illustrations for a hybrid power plant (solar plus battery) provided insights on the interaction of the DC resource and train profiles with the R-MVDC network and the impact of various parameters (e.g., converter ratings, bidirectionality, etc.) on the comparison.

Future work is directed to integrating the converter rating and the Joule losses costs in the DC resource optimization problem, further refining costs (e.g., HVAC network related costs) and benefits (e.g., from ancillary services), as well as the R-MVDC network model (e.g., several catenaries).

REFERENCES

[1] Z. Ma et. al, Medium voltage direct current (MVDC) grid feasibility study, Technical brochure TB793, CIGRE, Feb. 2020.

[2] J. Yu and J. Liang, Medium voltage DC distribution systems, Technical brochure TB875, CIGRE, July 2022.

[3] A. Verdicchio, P. Ladoux, H. Caron, and C. Courtois, "New medium-voltage DC railway electrification system," IEEE Trans. Transportation Electrification, vol. 4, no. 2, pp. 591–604, June 2018.

[4] H. Shigeeda, H. Morimoto, K. Ito, T. Fujii, and N. Morishima, "Feeding-loss Reduction by Higher-voltage DC Railway Feeding System with DC-to-DC Converter," The 2018 International Power Electronics Conference.

[5] J. P. Stovall et al., Comparison of costs and benefits for dc and ac transmission. Technical Report ORNL-6204, Oak Ridge National Lab, Oak Ridge, TN, Feb. 1987.

[6] Small-scale high voltage direct current. Technical report, Alaska Center for Energy and Power, June 2013.

[7] P. Le Métayer et al., "Break-even distance for MVDC electricity networks according to power loss criteria, 23rd Eur. Conf. Power Electronics Applications (EPE'21 ECCE Europe), pp. 1–9, Sep. 2021.

[8] L. Cornaggia, O. Despouys, H. Clémot, R. Girard and P. Andrianesis, Comparison of Losses and Costs between AC and MVDC Connections for New DC Resources, 2023 IEEE PES Innovative Smart Grid Technologies Europe (ISGT EUROPE).

[9] M. De Felice, ENTSO-E Pan-European Climatic Database (PECD 2021.3) in Parquet format [Data set]. Zenodo. https://doi.org/10.5281/zenodo.5780185, 2021.

This work is part of the RACCOR-D project, funded by the French government as part of France 2030.